# Supplementary Information 1

## SWAMNA: a comprehensive platform for analysis of nucleic acid modifications

Yixuan Xie,[a] Francisca N. De Luna Vitorino,[a] Ye Chen,[a] Joanna K. Lempiäinen,[a] Chenfeng Zhao,[b] Robert T. Steinbock,[c] Xingyu Liu,[a] Zongtao Lin,[a] Emily Zahn,[a] Arabella L. Garcia,[a] Matthew D. Weitzman,[c,d] and Benjamin A. Garcia,[a,*]

[a]Department of Biochemistry and Molecular Biophysics, Washington University School of Medicine, St. Louis, Missouri, United States.

[b]Department of Computer Science & Engineering, Washington University in St. Louis, St. Louis, Missouri, United States.

[c]Division of Protective Immunity and Division of Cancer Pathobiology, The Children's Hospital of Philadelphia, Philadelphia, PA, United States.

[d]Department of Pathology and Laboratory Medicine, Perelman School of Medicine, University of Pennsylvania, Philadelphia, PA, Unites States.

*Correspondence and requests for materials should be addressed to B.A.G. (bagarcia@wustl.edu).

## Method Details

**Cell culture.**

Malignant peripheral nerve sheath tumor (MPNST) cells, STS26T and S462, and human lung carcinoma A549 cells were all obtained from ATCC. Cells were grown in Dulbecco's Modified Eagle (DMEM) medium (Gibco, NY) supplemented with 10% (*v/v*) FBS (R&D Systems, MN), 1% Penicillin-Streptomycin (Gibco, NY) and 1% GlutaMAX (Gibco, NY). Cells were maintained in a humidified incubator at 37°C with 5% $CO_2$ and subcultured at 80% confluency.

**Adenovirus infections.**

The virus infection was performed as previously described.[1] Briefly, lung carcinoma epithelial A549 cells were mock infected or infected with WT Ad5 at MOI = 10 PFU/cell, in triplicates. Total RNA was extracted at 24- and 48-hours post-infection (hpi) with TRIzol (Thermo Fisher Scientific, MA) following the manufacturer's protocol.

**RNA and DNA extraction from cells.**

The RNA and DNA were extracted using TRIzol reagents. Briefly, the crude RNA and DNA were sequentially extracted from TRIzol reagents using chloroform and ethanol precipitation. The extracted total RNAs were subsequently treated with DNase I at room temperature for 15 minutes and protease K at room temperature for 30 minutes. RNA was further purified using RNA Clean & Concentrator (Zymo Research, CA). The purity of RNA was confirmed using nanodrop and Urea-TBE gel. Meanwhile, after removing remaining aqueous phase overlying the interphase, DNA was precipitated using ethanol. The crude extracted DNA was treated with 10 μg of RNase A for 30 minutes at 50°C, after which 20 μg of Proteinase K was added for another 30 minutes at

50°C. DNA was further purified with MinElute PCR purification kit (Qiagen, Netherlands) according to manufacturer instructions. The purity of DNA was confirmed using nanodrop.

**RNA and DNA digestion.**

RNA was digested using "one-pot" reaction as previously described.[2] Briefly, 1 μg of purified RNA samples were digested into nucleosides with 5 mU/μL of nuclease P1 (NP1), 5 mU/μL of recombinant shrimp alkaline phosphatase (rSAP), 500 μU/μL of phosphodiesterase I (PDE-I) and 6.25 μU/μL of phosphodiesterase II (PDE-II) in 20 μL of digestion buffer (1 mM $ZnCl_2$, 1 mM $MgCl_2$, 40 mM sodium acetate, pH 7.5) overnight at room temperature. The reaction was quenched with denature of RNase at 95°C for 10 minutes. The digested nucleosides were purified using Hypercarb SPE 96-well plates (Thermo Fisher Scientific, MA) and dried in a TurboVap LV Evaporators (Biotage, Sweden).

DNA samples were digested as previously described with some optimization.[3] Purified DNA (1 μg) was digested overnight at 37°C with 2.5U Supernuclease (SN), 0.02U PDE-I and 2U calf intestinal phosphatase in 20 μL of digestion buffer overnight at 37°C. The digested nucleosides were purified using Hypercarb SPE 96-well plates and dried in a TurboVap LV Evaporators.

**Permethylation of nucleosides.**

The digested ribonucleoside samples were permethylated using solid-phase permethylation, as previously described.[4] Briefly, NaOH beads were packed into the empty spin columns (about 2 cm height), and the beads were washed with 100 μL of DMSO twice. The purified and dried ribonucleoside samples were reconstituted in a mixture of 1 μL of water, 50 μL of DMSO, and 30 μL of iodomethane-$d_3$. The samples were loaded into the spin column and spun down at 200 x g, followed by reloading the samples into the column four times. Next, 20 μL of iodomethane-d3

was added to the sample and incubated at room temperature for another 10 min. The column was washed with 50 µL of DMSO twice, 500 µL of ice-cold water was added into the sample, and the mixture was incubated at room temperature for at least 1 min to quench the reaction. To extract the permethylated nucleosides, 300 µL of dichloromethane was added, the liquid−liquid extraction was repeated at least five times for each sample, and the organic layer was dried using a Savant SpeedVac concentrator.

**LC-MS/MS Analysis.**

The analysis of the nucleosides was carried out on a ZenoTOF 7600 system (SCIEX, MA) coupled to nanoAcquity UPLC System (Waters, MA). For the analysis, 2 µL of the sample was injected and separated using Waters nanoEase M/Z HSS T3 Column (300 µm X 150 mm, 1.8 µm) with a 20 min binary gradient with a constant flow rate of 10 µL/min. Mobile phase A was water with 0.1% (*v/v*) formic acid, and mobile phase B was ACN with 0.1% (*v/v*) formic acid. To analyze the underivatized nucleosides, the following binary gradient was used: 0−2 min, 0% B; 2−5 min, 0-6% B; 5−7 min, 6%-10% B; 7−9 min, 10%-30% B; 9−10 min, 30−80% B; 10−14 min, 80% B; 14−15 min, 80-0% B; 15−20 min, 0% B. To analyze the permethylated nucleosides, the following binary gradient was used: 0−1 min, 10% B; 1−7min, 10-40% B; 7−10 min, 40%-70% B; 10−11 min, 70%-99% B; 11−15 min, 90% B; 15−16min, 90%-10% B; 16−20 min, 10% B. The analytes were ionized using OptiFlow Turbo V ion source operated in the positive ion mode at 4500 V. Ion source gas1 and gas2 were at 20 and 60 psi, respectively. The ion transfer tube temperature and column temperature were set at 200°C and 45°C, respectively. The precursor ions were fragmented using collision-induced dissociation (CID) with optimized energy. zenoSWATH window was calculated

with optimization using SWATH Variable Window Calculator (v1.2), and the details were listed in Table S1-4. All data was collected using SCIEX OS software (v3.0).

**Data Analysis.**

For the manual inspection, the nucleosides were identified and quantified using OS Analyst (v1.7.3) and Skyline (v22.2).[5] NuMo Finder (https://github.com/ChenfengZhao/NuMoFinder) was used for automated identification and quantification. The heatmap was made using Mass Dynamics (massdynamics.com).

## Supplementary Figures

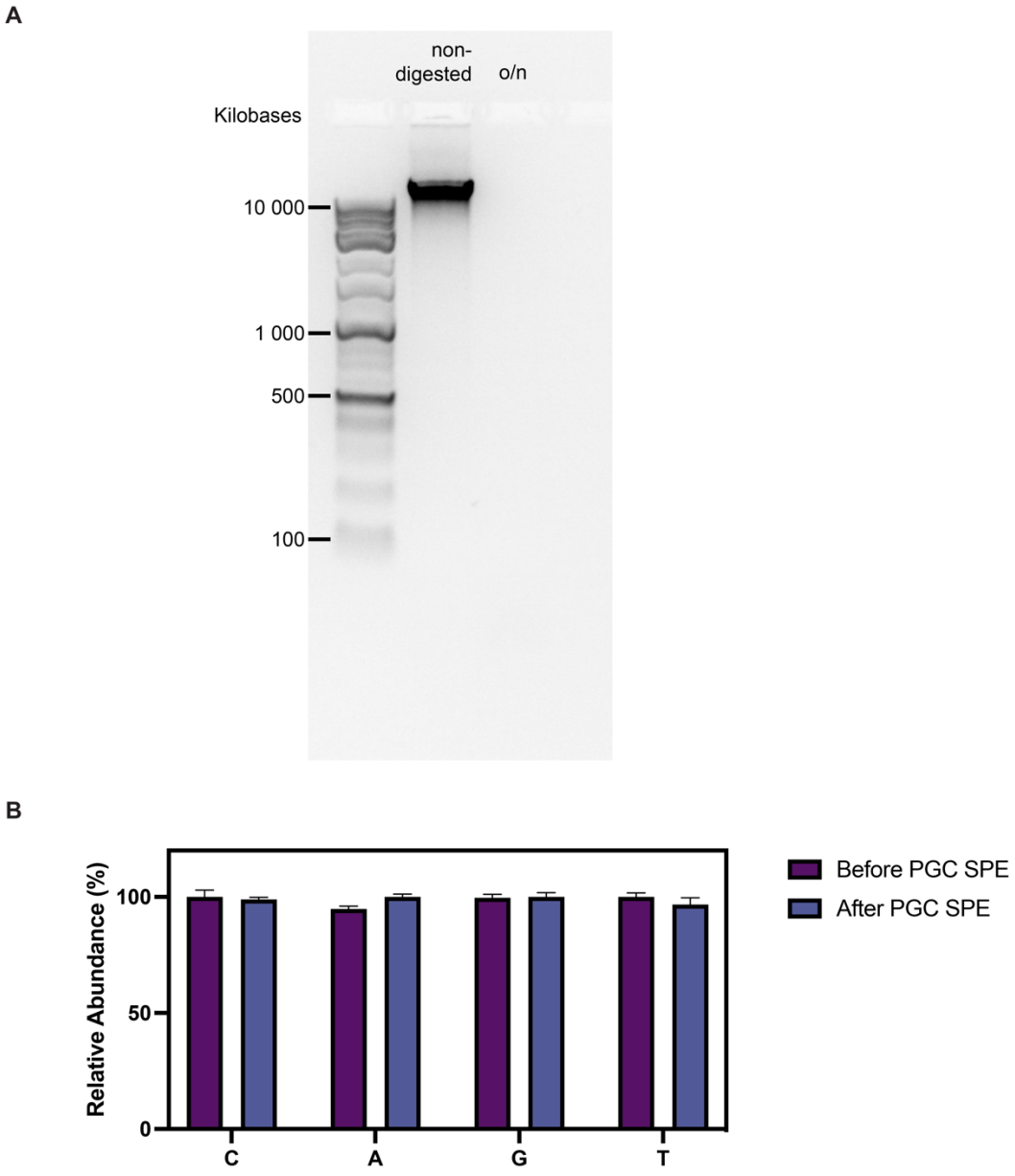


**Figure S1. Investigation of the effect of sample processing for DNA samples. (A)** Agarose gel (1% agarose-TAE gel) shows the complete digestion of DNA using a "one-pot" reaction. The first lane is 1μg of genomic DNA extracted from the STS26T cells. The second lane is 1μg of genomic DNA digested overnight as described in the method section. TriDye™ 1 kb Plus DNA Ladder is used as the reference. **(B)** Comparison of standard nucleosides before and after PGC SPE. The abundance is normalized to the abundance of standard before the purification. No significant losses are observed, confirming the capability of PGC SPE for deoxyribonucleoside clean-up.

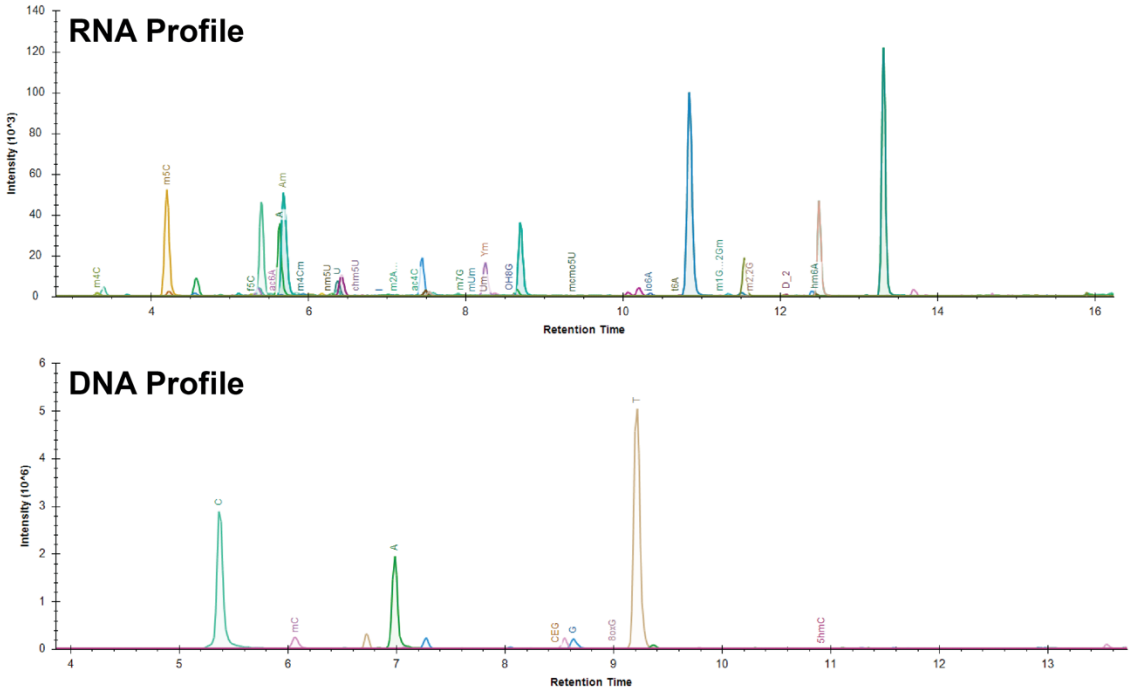


**Figure S2. The profile of nucleoside standards.** The permethylated nucleoside peaks are evenly distributed across the chromatogram in the reversed-phase C18 column. Annotation is based on Modomics and DNAmod databases.[6, 7]

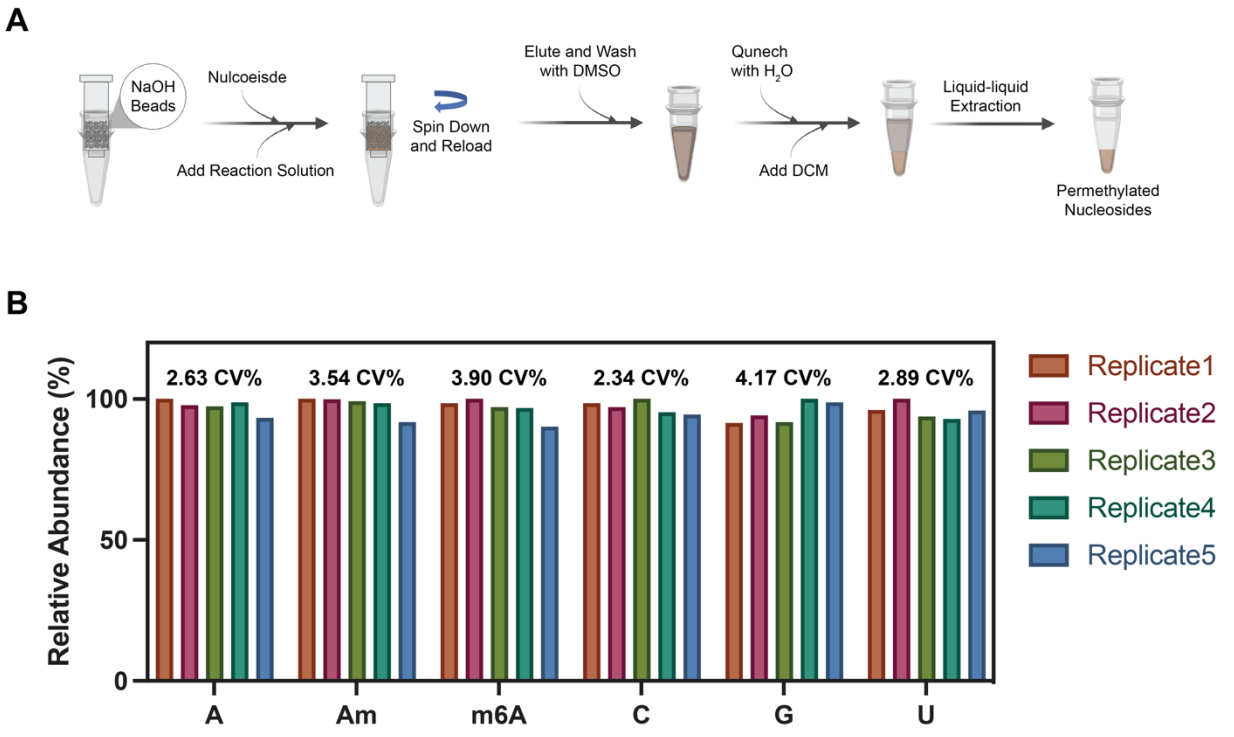


**Figure S3. Permethylation is used to derivatize the nucleoside molecules. (A)** The workflow of permethylation using the solid-phase reaction. **(B)** Five technical replicates of standard ribonucleosides from permethylation reaction were prepared. The abundance is normalized to the highest abundance within the sample. The coefficient of variation (CV)% is less than 5, and the results suggest the permethylation reaction in the SWAMNA platform is reproducible and stable.

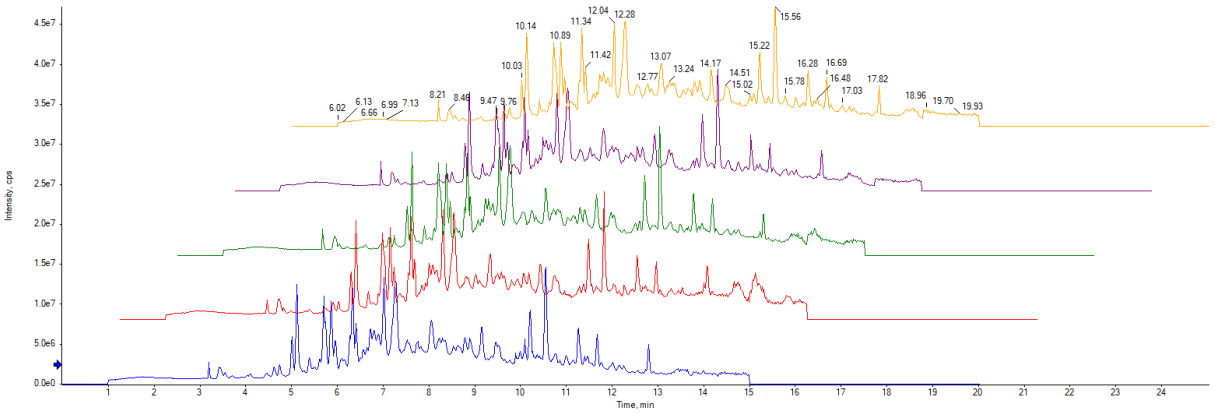


**Figure S4. Total ion chromatogram (TIC) of the zenoSWATH analysis.** Highly reproducible chromatograms, including retention time, major peaks, and peak abundance, are obtained in the SWAMNA platform.

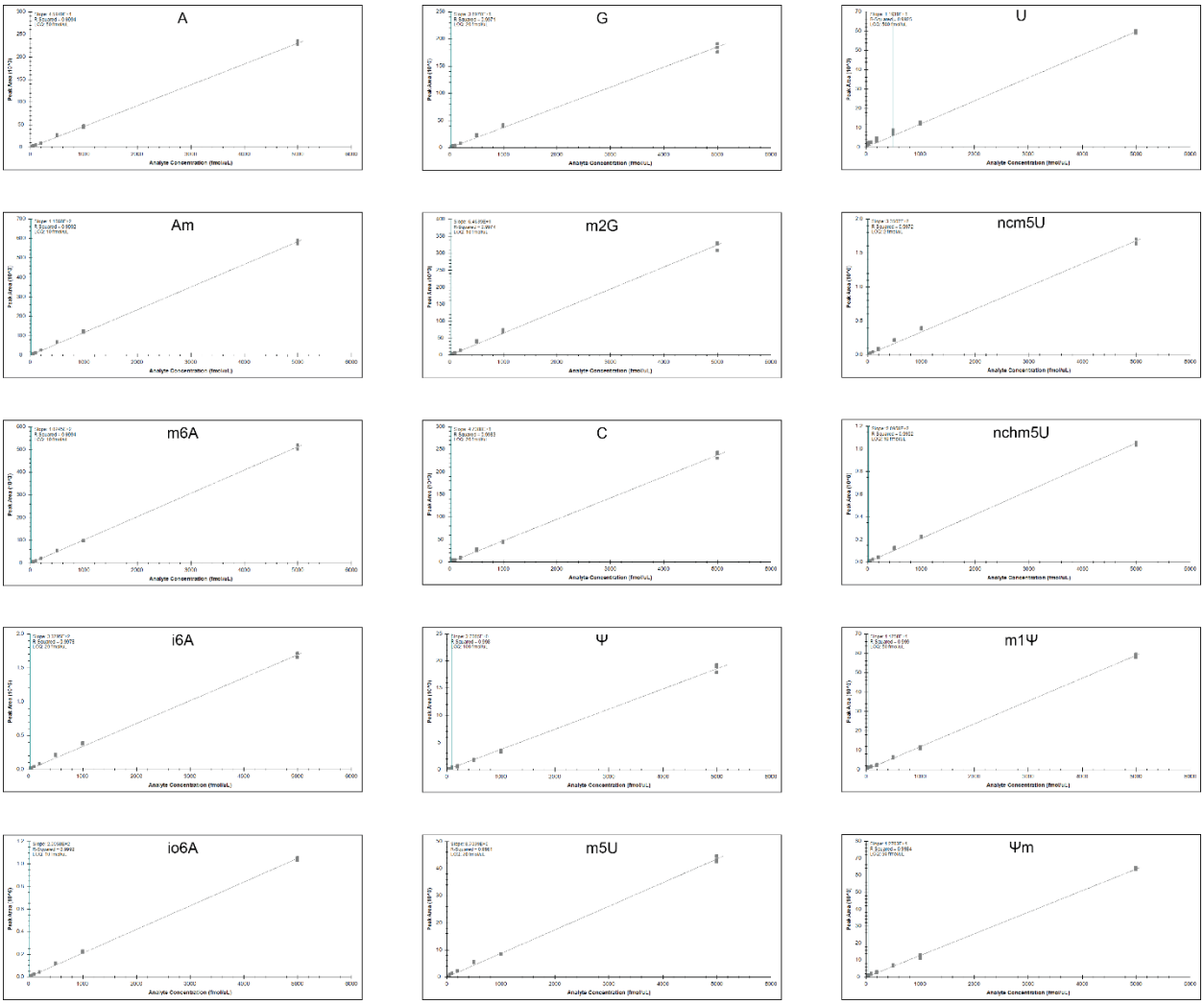


**Figure S5. Summary of calibration curve of permethylated nucleoside standards.** The coefficient of determination ($R^2$) for the nucleosides is more than 0.99, and indicates the very good linearity of the analysis in SWAMNA platform. The values are calculated using Skyline software.

.

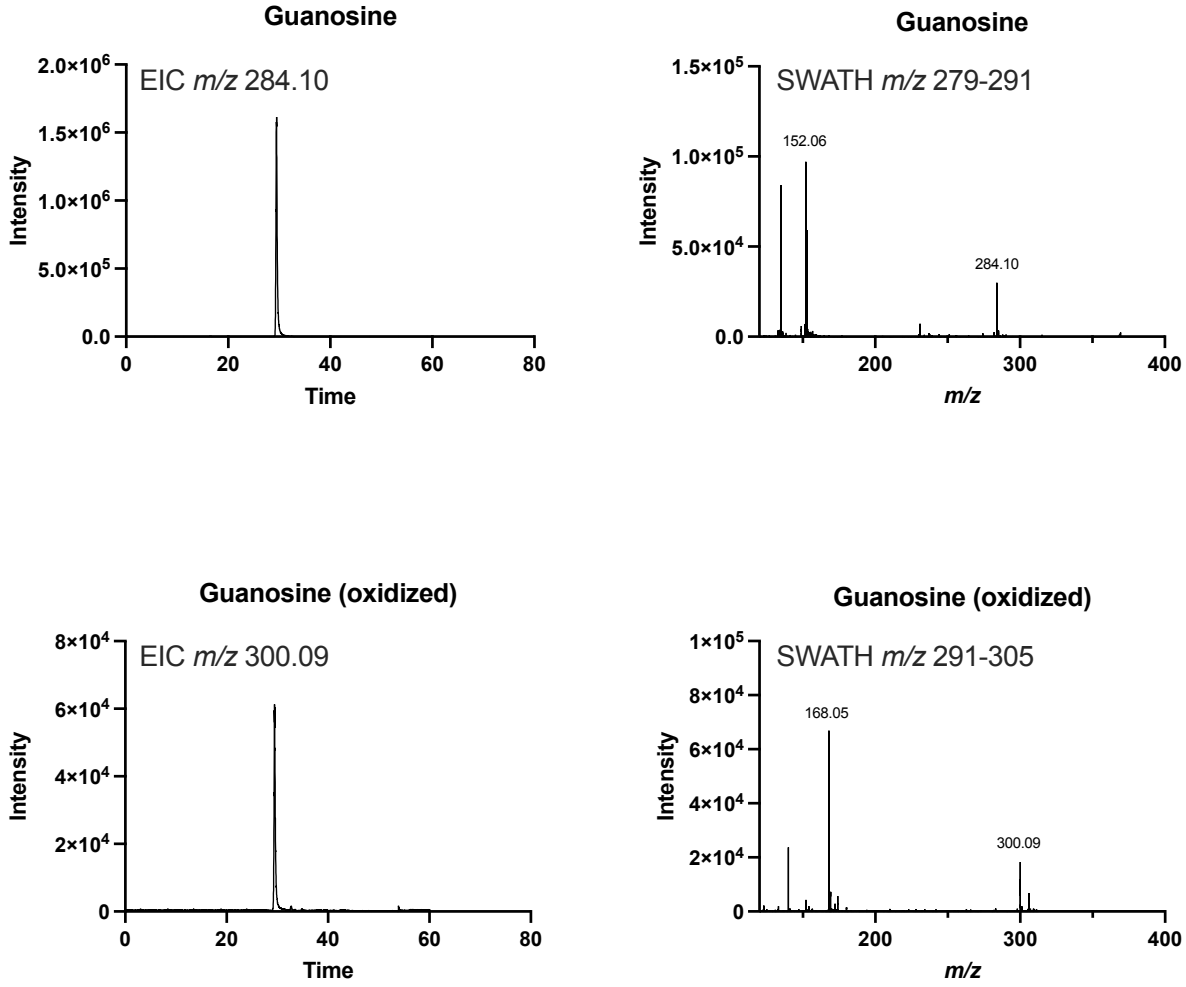


**Figure S6. Oxidized guanosines is identified using NuMo Finder.** The extracted ion chromatogram (EIC) of precursor ions and the SWATH MS/MS are shown. *m/z* at 284.10, 152.06, 168.05, and 300.09 corresponds to the guanosine, guanine, guanosine (+O), and guanine (+O).

## Supplementary Table

| *Scan Event* | *Ribonucleoside (native)* | *Deoxyribonucleoside (native)* | *Ribonucleoside (CD3)* | *Deoxyribonucleoside (CD3)* |
|---|---|---|---|---|
| MS1 | 200-1250 | 200-1250 | 250-1050 | 250-1050 |
| *MS2_1* | 240-264 | 223-247 | 305-312 | 271-278 |
| *MS2_2* | 264-278 | 247-261 | 312-322 | 278-288 |
| *MS2_3* | 278-291 | 261-274 | 322-328 | 288-294 |
| *MS2_4* | 291-305 | 274-288 | 328-336 | 294-302 |
| *MS2_5* | 305-319 | 288-302 | 336-349 | 302-315 |
| *MS2_6* | 319-339 | 302-322 | 349-356 | 315-322 |
| *MS2_7* | 339-373 | 322-356 | 356-364 | 322-330 |
| *MS2_8* | 383-415 | 366-398 | 364-369 | 330-335 |
| *MS2_9* | 415-450 | 398-433 | 369-375 | 335-341 |
| *MS2_10* | 449-485 | 432-468 | 375-382 | 341-348 |
| *MS2_11* | 484-520 | 467-503 | 382-389 | 348-355 |
| *MS2_12* | 519-555 | 502-538 | 389-402 | 355-368 |
| *MS2_13* | 554-590 | 537-589 | 402-417 | 368-383 |
| *MS2_14* | 589-625 | 589-625 | 417-426 | 383-392 |
| *MS2_15* | 624-670 | 624-670 | 426-437 | 392-403 |
| *MS2_16* | 659-695 | 659-695 | 437-461 | 403-427 |
| *MS2_17* | 694-730 | 694-730 | 461-485 | 427-451 |
| *MS2_18* | 729-965 | 729-965 | 485-534 | 451-500 |
| *MS2_19* | 764-800 | 764-800 | 534-574 | 499-540 |
| *MS2_20* | 799-835 | 799-835 | 574-618 | 574-610 |
| *MS2_21* | 834-870 | 834-870 | 618-650 | 609-645 |
| *MS2_22* | 869-905 | 869-905 | 649-685 | 644-680 |
| *MS2_23* | 904-940 | 904-940 | 684-720 | 679-715 |
| *MS2_24* | 939-975 | 939-975 | 719-755 | 714-750 |
| *MS2_25* | 974-1010 | 974-1010 | 754-790 | 749-785 |
| *MS2_26* | 1009-1045 | 1009-1045 | 789-825 | 784-820 |
| *MS2_27* | 1044-1080 | 1044-1080 | 824-860 | 819-855 |
| *MS2_28* | 1079-1115 | 1079-1115 | 859-895 | 854-890 |
| *MS2_29* | 1114-1150 | 1114-1150 | 894-950 | 889-925 |
| *MS2_30* | 1149-1200 | 1149-1200 | 949-1000 | 924-1000 |

**Table S1. SWATH windows for analyzing RNA and DNA modifications.**

## References


1. A. M. Price, K. E. Hayer, A. B. R. McIntyre, N. S. Gokhale, J. S. Abebe, A. N. Della Fera, C. E. Mason, S. M. Horner, A. C. Wilson, D. P. Depledge and M. D. Weitzman, *Nature Communications*, 2020, **11**, 6016.
2. K. A. Janssen, Y. Xie, M. C. Kramer, B. D. Gregory and B. A. Garcia, *Journal of the American Society for Mass Spectrometry*, 2022, **33**, 885-893.
3. W. Lai, C. Lyu and H. Wang, *Analytical Chemistry*, 2018, **90**, 6859-6866.
4. Y. Xie, K. A. Janssen, A. Scacchetti, E. G. Porter, Z. Lin, R. Bonasio and B. A. Garcia, *Analytical Chemistry*, 2022, **94**, 7246-7254.
5. K. J. Adams, B. Pratt, N. Bose, L. G. Dubois, L. St. John-Williams, K. M. Perrott, K. Ky, P. Kapahi, V. Sharma, M. J. MacCoss, M. A. Moseley, C. A. Colton, B. X. MacLean, B. Schilling and J. W. Thompson, *Journal of Proteome Research*, 2020, **19**, 1447-1458.
6. P. Boccaletto, F. Stefaniak, A. Ray, A. Cappannini, S. Mukherjee, E. Purta, M. Kurkowska, N. Shirvanizadeh, E. Destefanis, P. Groza, G. Avşar, A. Romitelli, P. Pir, E. Dassi, S. G. Conticello, F. Aguilo and J. M. Bujnicki, *Nucleic Acids Research*, 2022, **50**, D231-D235.
7. A. J. Sood, C. Viner and M. M. Hoffman, *Journal of Cheminformatics*, 2019, **11**, 30.